32nd URSI GASS, Montreal, 19–26 August 2017

Low-PAPR condition for 5G-candidate waveforms

Mouna BEN MABROUK, Marwa CHAFII, Yves LOUËT and Faouzi BADER
IETR/CentraleSupélec, Campus de Rennes, 35511 Cesson-Sevigné, France
{mouna.benmabrouk, marwa.chafii, yves.louet, faouzi.bader}@centralesupelec.fr

Abstract

To meet 5G networks challenges in terms of high data rates and spectral efficiency, one solution might be using multicarrier modulations (MCM)s. However, using MCMs is synonymous with low energy efficiency due to their high peak-to-average power ratio (PAPR). Indeed, high PAPR signals drive power amplifiers to operate most of the time in the linear zone. This latter corresponds to low power efficiency. This leads to a trade-off between spectral and energy efficiency. For this reason, PAPR reduction techniques have been highly addressed in literature. In this work, this trade-off is addressed differently: a necessary condition to achieve better PAPR performance than orthogonal frequency division multiplexing (OFDM) is established. This theoretical condition is verified by simulation results carried on Fourier-based and wavelet-based MCMs. The established condition classifies the MCMs into three categories regarding the PAPR: same as, higher than and lower than the OFDM PAPR level.

1 Introduction

Reducing the energy consumption is one of the main challenges of the next generation communication networks. Indeed, according to the statistics made on CO_2 emissions in 2007, from 2% to 4% are caused by the information and communications technology (ICT) industry [1]. This is due to the highly used electricity servers to produce the required energy for this field [2]. In ICT field, 90% of the consumed energy is used by the communications networks. Among these 90%, 80% are consumed by the base stations (BS). 60% of the consumed energy of CS is used by the power amplifier (PA) [3]. Therefore, to reduce the energy consumption in the ICT domain, we need to enhance the PA energy efficiency. However, another main objective of the 5G networks is ensuring high data rates and spectral efficiencies. To meet these targets, two solutions can be used:

1. To use a multicarrier modulation: in literature, several MCMs such as OFDM, universal filtered-OFDM (UF-OFDM), filtered-OFDM (F-OFDM), generalized frequency division multiplexing (GFDM) and filter bank multicarrier offset-QAM (FBMC-OQAM) are proposed. One common point between these MCMs is that they are Fourier transform based modulations. In addition, they have a high peak-to-average power ratio (PAPR). Having a high PAPR drives the PA to operate most of the time in its linear region which is a very low efficiency region. For this reason, PAPR reduction techniques are conventionally used [4, 5, 6].

2. To design a low PAPR MCM: In this paper, the second solution is addressed. Indeed, we focus on the PAPR criterion, and we investigate the behaviour of the PAPR regarding the modulation waveforms. It has been proved that the PAPR depends on the waveform used in the modulation in [7, 8]. Thus, one can change the PAPR performance by changing the characteristics of the waveform, which gives new insights regarding PAPR reduction.

In a previous work [9], it has been shown analytically that having a temporal support strictly less than the symbol period is a necessary condition on alternative waveforms with better PAPR than OFDM [9]. In addition, if the previous necessary condition is not satisfied, i.e if the waveforms have a temporal support larger than or equal to the symbol period, then their PAPR performance cannot be better than that of conventional OFDM. The studied MCMs in [9], are windowed cyclic prefix OFDM, non-orthogonal frequency division multiplexing, Walsh-Hadamard multicarrier, Haar-based wavelet-OFDM and Meyer-based wavelet-OFDM.

In this work, the study is extended to the analysis of the PAPR in UF-OFDM, GFDM, F-OFDM and FBMC-OQAM MCMs. This paper is organized as follows: In Section 2, the PAPR optimization problem as well as the solutions are briefly explained. The considered modulation schemes are presented and classified in Section 3. Finally, the paper conclusion is given in Section 4.

2 PAPR optimization

In this section, we consider the generalized waveforms for multicarrier (GWMC) system. This system represents a large set of modulation schemes.

2.1 System model

The GWMC transmitted signal is expressed as

$$s_k = \sum_{n\in\mathbb{Z}} \sum_{m=0}^{M-1} x_{m,n} \underbrace{g_m[k-nM]}_{g_{m,n}[k]}, \qquad (1)$$

where $x_{m,n}, n \in \mathbb{Z}, m \in [\![0, M-1]\!]$ are the transmitted symbols from a complex constellation, assumed to be independent and identically distributed with zero mean and variance σ_x^2, and $g_{m,n}[k]$ is the waveform filter, as depicted in Figure 1. Based on Lyapunov central limit theorem, Chafii

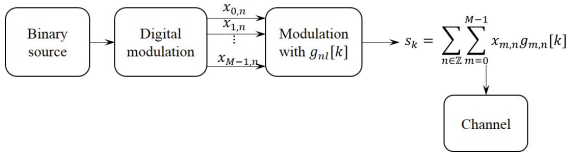

Figure 1. Multicarrier modulations general system model.

et al. proved in [7] that the PAPR complementary cumulative distribution function (CCDF) of these MCMs can be approximated as follows:

$$Pr(PAPR > \gamma) \approx 1 - \prod_{k \in [\![0, NM-1]\!]} (1 - e^{-c_k \gamma}), \qquad (2)$$

where

$$c_k = \frac{\sum_{n\in\mathbb{Z}} \sum_{m=0}^{M-1} |g_{m,n}[k]|^2}{N \sum_{m=0}^{M-1} |g_{m,n}[k]|^2},$$

and N is the number of MCMs frames considered in the observation and γ is the PAPR threshold. This expression is reliable when the following conditions are satisfied:

- About the input symbols: the real and imaginary parts of $(x_{m,n})_{(m\in[\![0,M-1]\!], n\in\mathbb{Z})}$ are independent and identically distributed.
- About the waveforms: $\{g_m\}_{m\in[\![0,M-1]\!]}$ are bounded and have a finite temporal support:

$$A := \min_{m,k} \sum_{n\in\mathbb{Z}} |g_{m,n}[k]|^2 > 0. \qquad (3)$$

  In other words, the temporal support of $g_{m,n}[k]$ has to be greater or equal to the symbol block period T i.e. containing M samples.
- About the subcarrier number: The number of subcarriers is supposed to be $M \geq 8$. This is an assumption made for the validity of the central limit theorem [7].

2.2 PAPR optimization problem

After establishing the PAPR CCDF expression, let us now build the PAPR optimization problem.

$$\begin{aligned} \underset{(g_m)_{m\in[\![0,M-1]\!]}}{\text{minimize}} \quad & Pr(PAPR > \gamma) \approx 1 - \prod_{k\in[\![0,NM-1]\!]} (1 - e^{-c_k\gamma}), \\ \text{subject to} \quad & A := \min_{m,t} \sum_{n\in Z} |g_{m,n}(t)|^2 > 0. \end{aligned}$$

Using the Riemann sum, it is straightforward to show that the PAPR optimization problem is equivalent to:

$$\begin{aligned} \underset{(g_m)_{m\in[\![0,M-1]\!]}}{\text{maximize}} \quad & \int_0^T \ln(1 - e^{\frac{-\gamma \sum_{m=0}^{M-1} \|g_m\|^2}{T \sum_{n\in\mathbb{Z}} \sum_{m=0}^{M-1} |g_{m,n}(t)|^2}})\, dt, \\ \text{subject to} \quad & A := \min_{m,t} \sum_{n\in Z} |g_{m,n}(t)|^2 > 0. \end{aligned}$$

2.3 Optimization problem solution

Let us now define as follows a critical value of γ, $\gamma_{\text{crit}}(\{g_m\})$, for a given GWMC:

$$\gamma_{\text{crit}}(\{g_m\}) := \sup_{t\in[0,T]} \frac{T \sum_{m=0}^{M-1} \sum_{n\in\mathbb{Z}} |g_{m,n}(t)|^2}{H_0 \sum_{m=0}^{M-1} \|g_m\|^2}. \qquad (4)$$

γ is assumed to be greater than or equal to $\gamma_{\text{crit}}(\{g_m\})$ and $H_0 = 0.63$ [9]. For a system satisfying (3) and having greater than or equal to $\gamma_{\text{crit}}(\{g_m\})$ and

$$\sum_{m=0}^{M-1} \sum_{n\in\mathbb{Z}} |g^*_{m,n}(t)|^2 \qquad \text{is constant over time.} \qquad (5)$$

For this system $\gamma_{\text{crit}}(\{g^*_m\}) = 1/H_0$ has the minimum possible value [7] and $\{g^*_m\}$ denotes the optimal $\{g_m\}$. In other words, the GWMC system $\{g^*_m\}$ has optimal PAPR performance at level γ among all GWMC systems satisfying (3) and $\gamma \geq \gamma_{\text{crit}}(\{g_m\})$.

The condition in (5) means that the statistical mean of the instantaneous power of the transmitted signal $E(|x(t)|^2)$ is constant over time. This condition is verified by OFDM systems. In addition, as, for an OFDM system, $\gamma_{\text{crit}}(\{g^*_m\}) = 1/H_0$, the OFDM is considered as an optimal solution for the optimization problem in subsection 2.2 [9].

We consider a GWMC system $\{g_m\}$ with $\gamma \geq \gamma_{\text{crit}}(\{g_m\})$. If this GWMC system has better PAPR performance at level γ than OFDM, then $\{g_m\}$ necessarily violates condition (3). Indeed, the fact that GWMC violates condition (3) means that the temporal support of at least one modulation function must be strictly smaller than the symbol period. Thus, we are led to a trade-off between frequency localization of multicarrier waveforms and PAPR performance.

3 Waveform classification regarding PAPR performance

In this section, we study the compliance of a set of MCMs with the conditions discussed in Section 2.3. This study is a comparison between wavelet-based, such as Haar and Meyer, and Fourier-based waveforms.

3.1 UF-OFDM

As illustrated by Figure 2, in UF-OFDM, the data symbols are assigned to each subcarrier in the allocated subcarrier set. Then, they are divided into B resource blocks (RBs). Each RB contains N_B consecutive subcarriers and consequently N_B data symbols. A M-point inverse discrete Fourier transform (IDFT) operation is performed for every RB to transform the frequency domain signal into time domain. The IDFT output signal of each sub-set is filtered by a Chebychev filter f^b of length L. The UF-OFDM signal is expressed as:

$$s_k = \sum_{b=0}^{B} \sum_{m=0}^{M-1} \sum_{p=(b-1)N_B}^{bN_B-1} x_{m,p} e^{j\frac{2\pi mp}{M}} f^b_{k-m}. \qquad (6)$$

As it can be seen from (6), the temporal support of the signal is larger than the symbol period. Therefore, the UF-OFDM might have the same or worse PAPR performance than the OFDM signal.

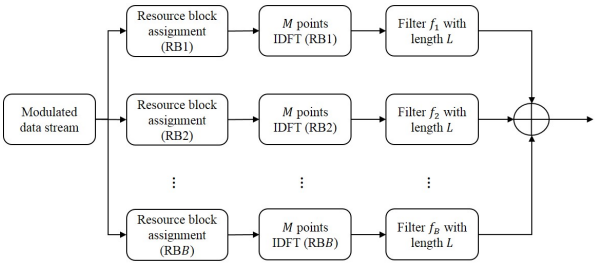

Figure 2. Generation of the UF-OFDM signal.

3.2 GFDM

GFDM is based on the time-frequency filtering of a data block, which leads to a flexible but non-orthogonal waveform. A data block is composed of K subcarriers and M time slots, and transmit $N = KM$ complex modulated data. Each data is filtered by a filter that is translated into both frequency and time domains. Thus, as the symbols overlap both in frequency and in time, interference (between sub-symbols and between symbols) occurs. To avoid inter-symbol interference, a CP is added at the end of each symbol of size KM. The GFDM waveform is parametrized by its shaping filter, which is usually chosen to be a Root Raised Cosine (RRC) filter [11]. The GFDM baseband transmitter block scheme is depicted in Figure 3. The GFDM signal is expressed as [11]:

$$s_k = \sum_{l=0}^{K-1} \sum_{m=0}^{M-1} x_{m,l} g[k-mN] e^{-j2\pi \frac{lk}{N}}, \qquad (7)$$

where the shaping filter $g[k-mN]$ is chosen to be circular with periodicity k mod MN, which is necessary to enable tail biting at the transmitter. As it is shown by (7), it is possible that the GFDM signal provides higher PAPR than the OFDM signal.

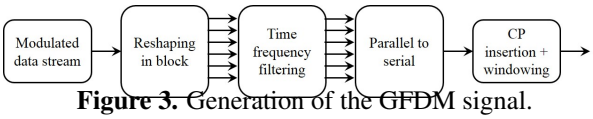

Figure 3. Generation of the GFDM signal.

3.3 FBMC-OQAM

The principle of FBMC is to use well-frequency localized prototype filters providing thus better adjacent channel leakage performance compared to OFDM. In order to ensure orthogonality between adjacent symbols and adjacent subcarriers, while keeping maximum spectral efficiency, Nyquist constraints on the prototype filter combined with OQAM are used. The FBMC-OQAM function is defined as [8]:

$$g_m(k-nN) = h_{OQAM}(k-nN) e^{(j2\pi \frac{m}{M}(k-D/2))} e^{j\theta_{m,n}},$$

then $|g_m(k-nN)|^2 = h^2_{OQAM}(k-nN)$, where h_{OQAM} is the prototype filter, D is the prototype filter overlapping factor and $\theta_{m,n} = \frac{\pi}{2}(m+n) - \pi mn$.

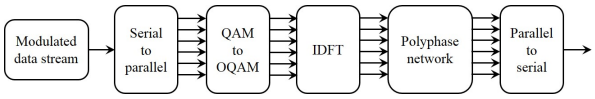

Figure 4. Generation of the FBMC-OQAM signal.

3.4 F-OFDM

As depicted in Figure 5, the F-OFDM signal is the conventional OFDM signal passed through an appropriately designed spectrum shaping filter [13]:

$$s_k = \sum_{l\in\mathbb{Z}} \sum_{l=0}^{M+Ng} \sum_{m=0}^{M-1} x_{m,n} f[k-mN] e^{j2\pi \frac{lk}{N}}, \qquad (8)$$

where N_g is the cyclic prefix length.

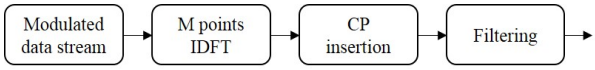

Figure 5. Generation of the F-OFDM signal.

The spectrum shaping filter f is centered in frequency at the assigned subcarriers. Its bandwidth is equal to the total frequency width of the assigned subcarriers, and its time duration is a portion of an OFDM symbol duration.

3.5 Waveform Classification

Other examples of multicarrier systems from the literature are also discussed such as Haar-based and Meyer-based wavelet-OFDM. For these latter, the reader may refer to [7, 9] to understand the waveforms structures. These MCMs have a temporal support smaller than the symbol period. They thus satisfy the necessary condition of having PAPR performance better than OFDM. For Haar-based wavelet-OFDM, only the condition (6) is verified which is not the case of the Meyer-based wavelet-OFDM.

The PAPR CCDFs of F-OFDM, GFDM, UF-OFDM and FBMC-OQAM are evaluated by simulations. The PAPR performance of these MCMs is shown by simulations to be higher than OFDM in Figure 6. This can be explained by the fact that these MCMs have a temporal support larger or equal to the symbol time. We understand now why FBMC systems based on PHYDYAS filter [12] as well as the UF-OFDM systems do not have better PAPR than OFDM, since they do not satisfy the necessary condition stated in Section 2.3. These simulations are carried over 7 symbol period signals using the signal parameters of Table 1. It should be noted that the PAPR performance of the GFDM is better than FBMC-OQAM. This is due to the considered simulation scenario. Indeed, the PAPR CCDF is calculated over only 7 symbols of M samples. The PAPR of the FBMC-OQAM is lower if it is calculated over a high number of symbols.

Figure 7 summarizes the conclusions of this study. The rectangle represents the set of all GWMC waveforms. The optimization problem analyzed in this work is for the waveforms belonging to the set A, which means satisfying (3). Systems in $A \cap B$ (including OFDM and F-OFDM) have

Table 1. Signal parameters

IDFT size: M	1024
Sub-set size: N_B	12
Sub-set number: B	18
Allocated subcarriers	216
Constellations	16-QAM
UF-OFDM: Filter	Chebychev
UF-OFDM: Filter length: L	72
UF-OFDM: Sidelobe attenuation	40 dB
GFDM: Filter	RRC
GFDM: sub-symbols number	7
F-OFDM: Filter	RRC
FBMC-OQAM: Filter	PHYDYAS

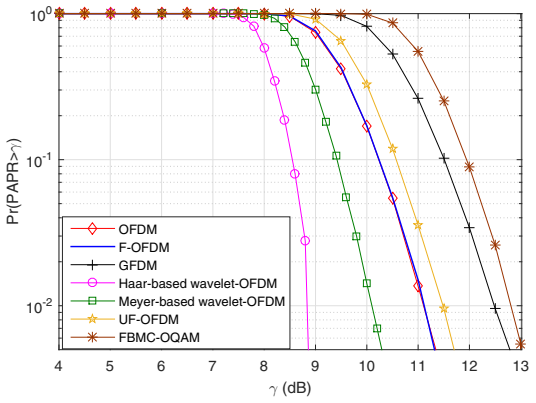

Figure 6. PAPR CCDF-based comparison between Fourier-based and wavelet-based MCMs.

the best possible PAPR performance *among all systems in A*. Any system with better PAPR performance than OFDM must be in C. There are indeed systems such as Meyer-based wavelet-OFDM in C with better PAPR performance than OFDM. Some are even in B (Haar wavelets), but not in A.

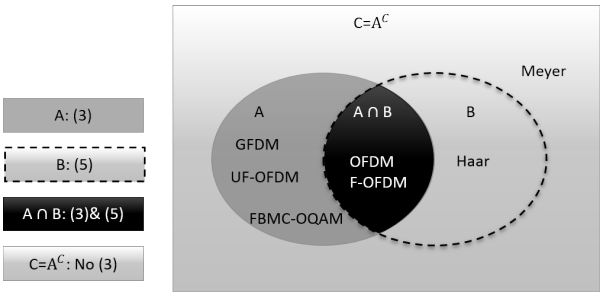

Figure 7. Classification of MCMs regarding the PAPR performance.

4 Conclusion

This paper is an extension of a previous work [9]. In this latter, it has been proved analytically that the PAPR, which depends on the modulation waveform, is optimal only if the sum of these waveforms over the number of carriers and the number of symbols is constant over time. In this paper, the relevance of this condition is validated by means of simulation results for GFDM, UF-OFDM, F-OFDM and FBMC-OQAM. In addition, the reason behind the high PAPR of these 5G candidate waveforms compared to OFDM is explained. The wavelet-based waveforms are verified to have the best PAPR.

Acknowledgements

This work is funded through the French National Research Agency (ANR) project WONG5 with grant: ANR-15-CE25-0005-03.

References

[1] J. G. Koomey, "Estimating total power consumption by servers in the US and the world," 2007.

[2] G. Fettweis and E. Zimmermann, "ICT energy consumption-trends and challenges," International Symposium on Wireless Personal Multimedia Communications, 2008.

[3] H. Bogucka and A. Conti, "Degrees of freedom for energy savings in practical adaptive wireless systems," IEEE Communications Magazine, vol. 49, no. 6, pp. 38-45, 2011.

[4] F. Tosato, M. Sandell and M. Tanahashi, "Tone reservation for PAPR reduction: An optimal approach through sphere encoding," 2016 IEEE International Conference on Communications (ICC), Kuala Lumpur, pp. 1-6, 2016.

[5] W. Wang, M. Hu, Y. Li, H. Zhang, "A low-complexity tone injection scheme based on distortion signals for PAPR reduction in OFDM systems," IEEE Transactions on Broadcasting, no. 06, pp. 1-9, 2016.

[6] J. Mountassir, A. Isar and T. Mountassir, "Precoding techniques in OFDM systems for PAPR reduction," IEEE Mediterranean Electrotechnical Conference, pp. 728-731, 2012.

[7] M. Chafii, J. Palicot, R. Gribonval, "Closed-form approximations of the peak-to-average power ratio distribution for multi-carrier modulation and their applications," EURASIP Journal on Advances in Signal Processing, vol. 2014, no. 01, 2014.

[8] A. Skrzypczak, *Contribution à l'étude des modulations multiporteuses OFDM/OQAM et OFDM suréchantillonnées*, PhD thesis, Rennes 1 University, France, 2007.

[9] M. Chafii, J. Palicot, R. Gribonval and F. Bader, "A Necessary Condition for Waveforms With Better PAPR Than OFDM," IEEE Transactions on Communications, vol. 64, no. 8, pp. 3395-3405, 2016.

[10] G. Fettweis, M. Krondorf, and S. Bittner, "GFDM - generalized frequency division multiplexing," IEEE Vehicular Technology Conference (VTC), pp. 1-4, 2009.

[11] N. Michailow, I. Gaspar, S. Krone, M. Lentmaier, and G. Fettweis, "Generalized frequency division multiplexing: Analysis of an alternative multi-carrier technique for next generation cellular systems," International Symposium on Wireless Communication Systems (ISWCS), pp. 171-175, 2012.

[12] M. G. Bellanger, "Specification and design of a prototype filter for filter bank based multicarrier transmission," International Conference on Acoustics, Speech, and Signal Processing (ICASP) pp. 2417-2420, 2001,

[13] J. Abdoli, M. Jia and J. Ma, "Filtered OFDM: A new waveform for future wireless systems," International Workshop on Signal Processing Advances in Wireless Communications (SPAWC), pp. 66-70, 2015.